The radio continuum spectrum of Centaurus A's large-scale components

H. Alvarez[1], J. Aparici[1], J. May[1], and P. Reich[2]

[1] Departamento de Astronomía, Universidad de Chile, Casilla 36-D, Santiago, Chile
[2] Max-Planck-Institut für Radioastronomie, Auf dem Hügel 69, 53121 Bonn, Germany

Abstract. Using our own observations at 45 MHz and data found in the literature after an exhaustive search, we have attempted a comprehensive study of the integrated flux density spectrum of the Centaurus A radio galaxy and of its large scale components. The spectrum for the whole object, between 10 and 4750 MHz, can be well represented by a power law with a spectral index of -0.70 ± 0.01, disproving the existence of a spectral break reported by other authors in the past. Between 406 and 4750 MHz we present, for the first time, the spectra of the individual Giant Outer Lobes and find that, within the errors of measurement, their spectral indices are practically equal. We show that the Giant Outer Lobes contribute with 73% of the total luminosity of the object. That the indices of the different large scale components are close or equal supports the double injection hypothesis for their origin. We discuss the spectral indices and luminosities, and we determine upper bounds for the ages of the radiating electrons. We show that Centaurus A supports the P-α rather than the z-α correlation.

Key words: galaxies: individual: NGC 5128 = Cen A – galaxies: active – radio continuum: galaxies

1. Introduction

Centaurus A (IAU 13S4A, NGC 5128, B1322$-$428, J1325$-$4303) is the strongest extragalactic radio source in the southern hemisphere and, being the closest radio galaxy to us, its structure can be studied in detail. It is an extended, complex and fairly symmetric source that exhibits two Giant Outer Lobes (GLs), the northern one (GLN) and the southern one (GLS), that span declinations between approximately $-38°$ and $-48°$. Closer to the center are two smaller Inner Lobes (ILs), situated to the northeast and southwest of the center, which we will designate as ILNE and ILSW, respectively. Approximately to the north of the ILNE is the Northern Middle Lobe, which has no symmetric counterpart in the south. The large feature between approximately $-38°$ and $-40°$ has been called the Northern Loop in the literature (Junkes et al. 1993). In the nuclear region are the nucleus, the jet, the counter jet and the knots. Good

Send offprint requests to: H. Alvarez

descriptions on Cen A morphology are found in Burns et al. (1983) and in a recent review by Israel (1998). Fig. 1 presents a 4.75 GHz map showing clearly all the large scale features of this radio galaxy. Some authors refer to the ILs plus the region closer to the center as the *central source* or as the *central component*. Also some authors refer to the GLs as the *extended source* or simply as the *outer lobes*. The morphological definitions we will use are as follows:

1. the *Whole Source* is Cen A in its entire extension,
2. the *Inner Lobes* (ILs) follow the usual definition, where ILNE indicates the inner lobe in the NE direction and ILSW in the SW direction, respectively,
3. the region internal to the ILs will be called *Nuclear Region* (NR),
4. the NR plus the ILs will be designated as the *Central Region* (CR),
5. the *Giant Northern Lobe* (GLN) comprises the region north of the center ($\delta \sim -42°45'$) less the corresponding part of the CR; thus the GLN includes the Northern Middle Lobe and the Northern Loop,
6. the *Giant Southern Lobe* (GLS) comprises the region south of the center less the corresponding part of the CR.

In what follows whenever we refer to a spectrum we will mean an *integrated flux density* spectrum. In the radio range the source has been observed between 4.7 MHz and 43 GHz by several authors; however, few of them have studied the spectrum of the Whole Source and none has attempted to investigate that of the individual GLs. The spectrum of the individual ILs has been well studied.

There are a number of discrepancies regarding the spectral index of the Whole Source. The first to investigate the spectrum of Cen A were Roman & Haddock (1956), although they failed to explicitly state the components of Cen A's emission considered in their study. Between 60 and 3200 MHz they found a discontinuity that resembled two straight segments with approximately the same index ($\alpha = -1.0$, with $S \sim \nu^{\alpha}$) but shifted in frequency, thus forming a sort of plateau around 500 MHz. A different result was obtained, in a seminal paper on the subject, by Cooper et al. (1965). These authors found a strong, positive curvature in the spectrum (i.e. a spectrum with negative index, that steepens with decreasing frequency) between 19.7 and 1410
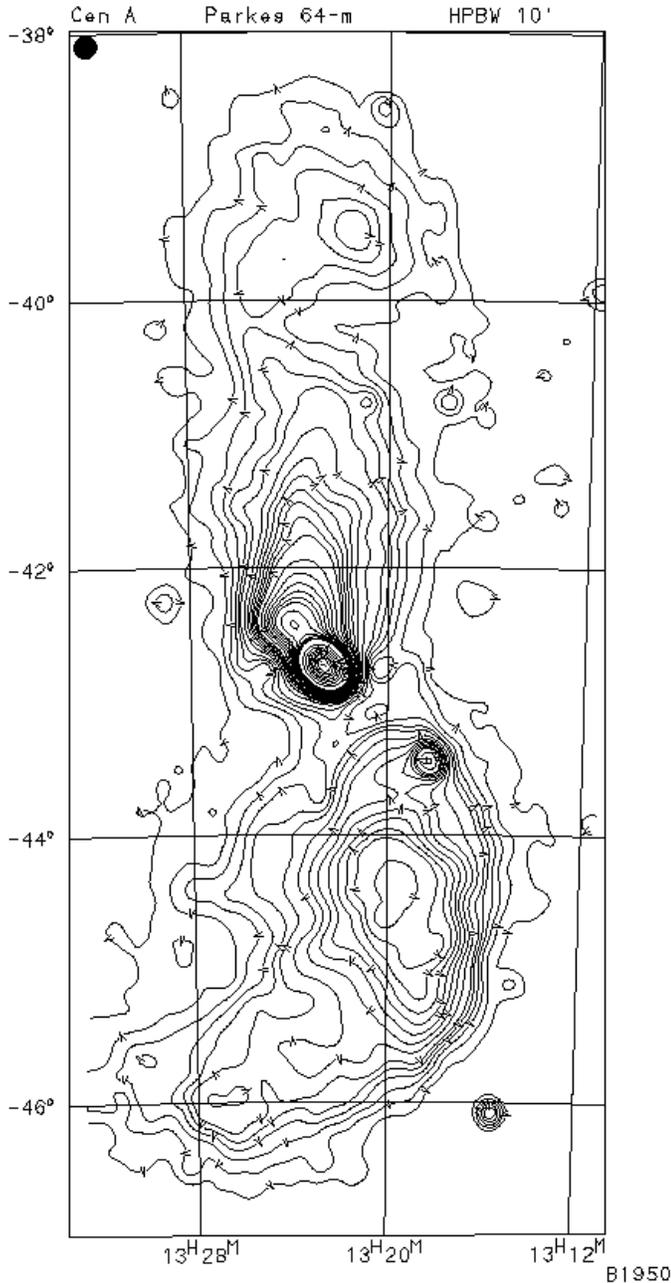
Fig. 1. Map of Centaurus A at 4.75 GHz (Junkes et al. 1993), smoothed to a resolution of $10'$. The temperature contours are not indicated since the purpose of the figure is to show the morphology of the object. All large scale components are clearly visible: the Northern Loop ($-40° \leq \delta \leq -38°$), the Northern Middle Lobe ($-42.5° \leq \delta \leq -41°$), the Central Region ($-43° \leq \delta \leq -42.5°$), the GLS ($\delta \leq -42.7°$), and the GLN ($\delta \leq -42.7°$)(see text)

MHz. The discrepancies between these two works emphasize that well-defined spectra of the whole source and of its components are important in studying the origin and evolution of the object. The first purpose of this paper is an attempt to resolve these discrepancies.

In the literature there is a great variety of values for flux densities and spectral indices for the different components of

Cen A. There is even confusion about the nomenclature, particularly regarding the smaller components. Partly for this reason we have made a careful and exhaustive study of the published material related to the Inner Lobes. This has also been necessary in order to compare the parameters of these lobes with those of the Whole Source and Giant Outer Lobes. Since we are interested in the study of the flux density of the large scale structures of Cen A we have made an attempt, for the first time, to determine the spectrum of the individual Giant Lobes. This is the second purpose of this paper.

To investigate the spectrum of the large scale components of Cen A we use our own observations at 45 MHz, the measurements at other frequencies found in the literature, and the determinations made by us from the data published by other authors. We compare the spectrum of the different components and briefly discuss them in relation to their origin and evolution.

2. The data

The 45-MHz observations have been made with the large array of the University of Chile as a part of the Southern Sky Survey (Alvarez et al. 1997). The antenna is a filled array of 528 full-wave dipoles oriented E-W, and has a resolution of $4°6\,(\alpha)$ x $2°4\,(\delta)$. A detailed description of this instrument can be found in May et al. (1984) and Alvarez et al. (1994). The contour map of Cen A, corrected for antenna sidelobes, can be seen in the 45 MHz survey (Alvarez et al. 1997, Fig. 1, p. 320). The source's multiple-lobe structure, readily seen in observations with higher resolution (Fig. 1), is lost in our data because of the instrument's low resolution. As a check of our observations, the data of Cen A at 408 MHz, from the all-sky survey of Haslam et al. (1982), was convolved to our antenna beam resulting in a map almost identical in morphology.

2.1. The total integrated flux density at 45 MHz

The flux densities of extended components have been computed graphically following the standard method of integrating brightness temperature contour maps (e.g. Bracewell 1962, Kraus 1966, Cooper et al. 1965). Since the sources are irregular in shape, the integrals are replaced by summations. There are four main sources of error in this calculation. The first one is the replacement of an integral by a summation; here the closer the contours, the better the approximation. The second one arises from the necessity to close open contours which are usually the external ones and correspond to the lower temperatures, so the error is not expected to be large. The third one is a possible temperature scale error present in the data, and which is usually given by the original authors. And the fourth one is the determination of the limits of the source, or base contour, which is usually not shown in the maps; however, the first contour given corresponds to a low relative temperature so the contribution from the region between the unknown base contour and the first contour is expected to be small. Obviously, the flux calculated from the first contour represents only a lower bound. To estimate this error we have assumed that the area between the base

and first contours is the same as that between the first and second contours. This is reasonable unless the temperature gradient changes significantly near the edge of the source.

The 45-MHz map was obtained by removing the background from the original data (Alvarez et al. 1997), using the so-called method of unsharp masking (Sofue & Reich 1979). Due to nearby features, not belonging to the source, a few external contours did not close; however, we did close them reasonably well by following the general trend of adjacent contours. We estimate the error in this process to be less than 10%. Regarding the error associated with the separation of the temperature contours, a first integration was done with a separation of 1000 K, then we repeated the process with 500 K and found a difference of 0.4%. We also found that adopting a base isophote of 500 K, instead of 0 K, yielded an error of 0.7%. Since the error in temperature scale of the Southern Survey (Alvarez et al. 1997) is better than 10%, we have adopted a total error of 15% for the 45-MHz integrated flux density of the Whole Source, which is 14900 ± 2200 Jy.

2.2. Integrated flux densities at other frequencies

From brightness temperature maps, made at different frequencies by other authors, we have computed the integrated flux density of some Cen A components. By graphical integration we determined the flux density of the individual GLs and of the Whole Source at 2650 MHz from Figs. 6(a) and 7(a) in Cooper et al. (1965). Table 1 lists the integrated flux densities of the Whole Source.

The absolute flux densities are extremely difficult to measure, especially at frequencies below 100 MHz where the problems are multiple and severe. The errors of measurement are not always given in the literature by the original authors and, whenever given, the type of error is not specified.

When we have found no error quoted by the original authors or by related works, we have estimated an appropriate value based upon the details of the observation and other available information. For example, Shain (1959) gives an error of 15% at 19.7 MHz (see Table 1). We estimate that the error must be larger at lower frequencies and so we have assigned an uncertainty of 20% to the measurements of Hamilton & Haynes (1968) at 10.0 MHz and Ellis & Hamilton (1966) at 4.7 MHz. In other cases we have adopted different criteria. To assign an error to the 406 MHz total flux of Cooper et al. (1965), we note that the southern survey made by Haslam et al. (1981) at 408 MHz using the same antenna (64-m Parkes Telescope) has a temperature scale error of probably better than 10%, so we have adopted this value. Similarly, we have used the temperature scale errors of the southern surveys by Hill (1968) at 1410 MHz and by Day et al. (1972) at 2700 MHz, also using the Parkes Telescope, to estimate the uncertainties in the measurements of Cooper et al. (1965) at 1410 and 2650 MHz. We have determined these to be 5 and 10%, respectively. To estimate the error in Bolton & Clark's (1960) observations at 960 MHz, we have used the value quoted by Harris & Roberts (1960) in an unrelated work at the same frequency and with the same antenna. In the case of our

Table 1. Integrated flux density of the Whole Source

ν (MHz)	S (Jy)	Reference
4.7	51000 ± 10200[a]	Ellis & Hamilton (1966)
10	43000 ± 8600[a]	Hamilton & Haynes (1968)
19.7	28000 ± 5600[b]	Shain (1959)
45	14900 ± 2200	This work
85.7	8700 ± 1300	Sheridan (1958)
406	2857[c] ± 428	Cooper et al. (1965)
408	2762 ± 370	Haslam et al. (1981)
843	1790 ± 161	Jones & McAdam (1992)
960	1676[d] ± 126	Bolton & Clark (1960)
960	2010 ± 150	Harris & Roberts (1960)
1410	1330 ± 133	Cooper et al. (1965)
2640	912 ± 9.1	Rogstad & Ekers (1969)
2650	728 ± 109	This work[e]
4750	579 ± 58[f]	Junkes et al. (1993)

[a] Error quoted is an estimate only.
[b] Error quoted by Cooper et al. (1965).
[c] Corrected by Haslam et al. (1981) using Baars et al.'s (1977) temperature scale.
[d] Corrected by Cooper et al. (1965).
[e] Based on data from Cooper et al. (1965). The error is the sum of: 3% from graphical integration, 2% from closing open contours, and 10% assumed from the brightness temperature scale.
[f] The original data have been reduced by 15% by indication of the authors (Junkes, personal communication). The error includes 5% uncertainty in the temperature scale.

determination at 2650 MHz, we have added to the temperature scale error the error derived from the graphical integration.

The extragalactic radio source PKS B1318−434 is seen projected on the GLS (Fig. 1). There has been some debate about this source being a hot spot of Cen A (see Junkes et al. 1993). This is a complex radio source and from the available information it seems likely that it is associated with the interacting system NGC 5090−5091 (Smith & Bicknell 1986; Jones & McAdam 1992). Since the contribution of this source to the flux of Cen A is only a fraction of 1% we have made no corrections for it.

We are aware that, to cover the widest range of frequencies, we have had to use results from many different types of instruments. The use of interferometric techniques is of particular concern in the determination of integrated flux densities for very extended sources, like Cen A. This is because extended sources can present large properties of their flux at low spatial frequencies, which are often sampled poorly by interferometers. Of the fourteen measurements presented in Table 1, four were obtained through interferometric methods (Shain 1959; Sheridan 1958; Jones & McAdam 1992; and Rogstad & Ekers 1969). The rest were observed with either single dishes or filled arrays.

Table 1 contains observations made not only with a variety of instruments, but also spanning 40 years. In fact, the majority of the observations were made during the 50's and 60's, particularly those at low frequencies. High quality observations

Table 2. Integrated flux density of the Inner Lobes

ν (MHz)	S_{ILNE} (Jy)	S_{ILSW} (Jy)	Reference
80	$1000^a \pm 90$	$680^a \pm 90$	Lockhart & Sheridan (1970)
80	$942^a \pm 94$	$640^a \pm 64$	Slee (1995)
160	$620^a \pm 81$	$484^a \pm 63$	Slee (1995)
327	417 ± 62	301 ± 45	Slee et al. (1983)
408	332 ± 33^b	238 ± 24^b	Cameron (1971)
843	220 ± 26	154 ± 18	Slee et al. (1983)
1415	120 ± 24	95 ± 19	Christiansen et al. (1977)
3300	102 ± 25	58 ± 15	Little et al. (1964)
5000	71 ± 18	55 ± 14	Cooper et al. (1965)
10700	24 ± 1.8	19.3 ± 1.4	Price & Stull (1973)
22000	20.2 ± 2.0^b	15.1 ± 1.5^b	Tateyama & Strauss (1992)
43000	11.9 ± 1.2^b	8.5 ± 0.9^b	Tateyama & Strauss (1992)

[a] Deduced from peak ratio.

[b] Error quoted is an estimate only.

Table 3. Integrated flux density of the Giant Outer Lobes

ν (MHz)	S_{GLN} (Jy)	S_{GLS} (Jy)	Reference
406	1075 ± 215^a	1070 ± 214^a	Cooper et al. (1965)
406	768 ± 154^b	1013 ± 152^c	This work[d]
960	$508^e \pm 38$	$731^e \pm 55$	Bolton & Clark (1960)
1410	510 ± 102^a	532 ± 106^a	Cooper et al. (1965)
1410	477 ± 95^b	565 ± 85^c	This work[d]
2650	269 ± 46^f	307 ± 34^g	This work[d]
4750	182 ± 42^h	229 ± 25^h	Junkes et al. (1993)

[a] Error quoted is an estimate only.

[b] The error is the sum of: 10% from graphical integration, and 10% assumed from the brightness temperature scale.

[c] The error is the sum of: 5% from graphical integration, and 10% assumed from the brightness temperature scale. [d] Based on data from Cooper et al. (1965).

[e] As corrected by Cooper et al. (1965).

[f] The error is the sum of: 7% from graphical integration, and 10% assumed from the brightness temperature scale.

[g] The error is the sum of: 4% from graphical integration, and 10% assumed from the brightness temperature scale.

[h] The original data have been reduced by 15%, by indication of the authors (Junkes, personal communication). The error includes 5% uncertainty in the temperature scale.

at frequencies below 100 MHz are especially difficult to perform, mainly because of ionospheric effects and interference from both natural and artificial sources. In Fig. 2 we see that, in spite of the uncertainties introduced by the use of so many different types of instruments, the fit of the mean values is good (correlation coefficient 0.998).

Table 2 shows the integrated flux densities of the ILs, collected from the literature. The situation in Table 2 is different because the Inner Lobes are small in angular size, and so only three of the twelve measurements were obtained with filled aperture instruments (Cooper et al. 1965; Tateyama & Strauss 1992).
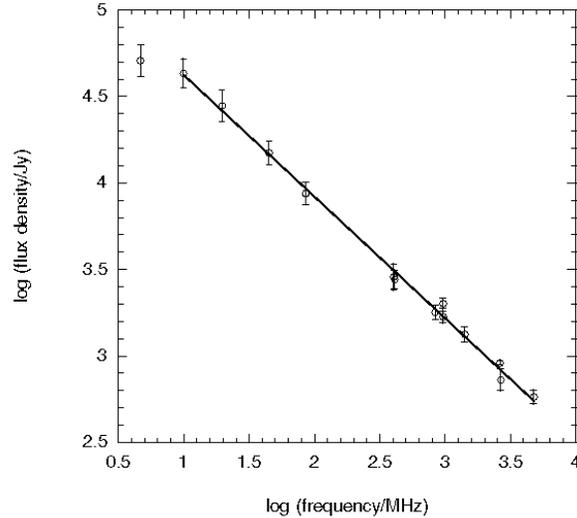
Fig. 2. Integrated flux density spectrum of Cen A (Whole Source). The straight line represents the least-squares fit to the data, given by the equation $\log S = (5.33 \pm 0.04) - (0.70 \pm 0.01) \log \nu$. The fit does not include the point at 4.7 MHz since it shows indications of absorption

In Tables 1 and 2 we have tried to avoid duplications between the original flux determinations and those presented in catalogues and compendia. Neither have we attempted to standardize flux density scales; however, we have used revised values whenever available.

The fluxes of the GLs, presented in Table 3, were obtained from observations made with large dishes; however, there are fewer data. Here the uncertainties are larger mainly because of the need to separate the GLs and the Central Region (CR). This is especially the case at the lower frequencies where the resolution is less. The GLs' contours near the CR were interpolated reasonably well by following the external shapes, far from the CR. Also, we checked that the sum of the three parts (GLN, GLS, CR) closely approximated the flux of the Whole Source as derived by us. This is the first time that a determination of the spectrum of the individual GLs has been attempted.

3. Discussion

3.1. The spectrum of the Whole Source

McGee et al. (1955) found a strong positive curvature in the spectrum of Cen A below about 1000 MHz, as did Cooper et al. (1965) who also claimed that the spectrum steepens with decreasing frequency. The fact that any significant deviation from a synchrotron spectrum has physical implications for either the source or the intervening medium (or both), prompted us to undertake an exhaustive study of the spectrum of Cen A. Furthermore, the spectrum has been studied thus far over a rather narrow range of frequencies. The present work, incorporating data found in the literature, extends this range from 1420 up to 4750 MHz. Table 4 gives the spectral indices for the Whole Source determined by different authors. Fig. 2 shows the spectrum of the Whole Source between 4.7 and 4750 MHz. Above 4.7 MHz the fluxes fit well a power law with spectral index

Table 4. Spectral index of the Whole Source

ν range (MHz)	α $S \sim \nu^{\alpha}$	Reference
$10 - 4670$	-0.70 ± 0.01	This work
$18.3 - 630$	-1.0	Shain (1958)
$19.7 - 405$	-0.9	Cooper et al. (1965)
$19.7 - 960$	-0.7	Bolton & Clark (1960)
$86 - 1423$	-0.67	Goldstein (1962)
$400 - 1400$	-0.72	Heeschen (1960)
$405 - 1420$	-0.6	Cooper et al. (1965)

Fig. 3. Integrated flux density spectrum of the Inner Lobes. The straight lines represent the least-squares fits to the data corresponding to the NE and SW lobes, as given by the equations $\log S_{\mathrm{ILNE}} = (4.35 \pm 0.08) - (0.70 \pm 0.02) \log \nu$ and $\log S_{\mathrm{ILSW}} = (4.19 \pm 0.06) - (0.70 \pm 0.02) \log \nu$, respectively

-0.70 ± 0.01, and a correlation coefficient of 0.998. Below 10 MHz there are indications of absorption, as already noticed by Ellis & Hamilton (1966), so the straight line spectrum could be extrapolated down to 4.7 MHz (Hamilton & Haynes 1968). We see that Table 4 contains a spread of values for the spectral index of the Whole Source, ranging approximately between -0.6 and -1.0. This spread in results is probably attributable to the reduced frequency range or to the insufficient number of observed frequencies comprising each measurement.

To obtain the fitted spectra presented in this work all of the data points were given equal weight.
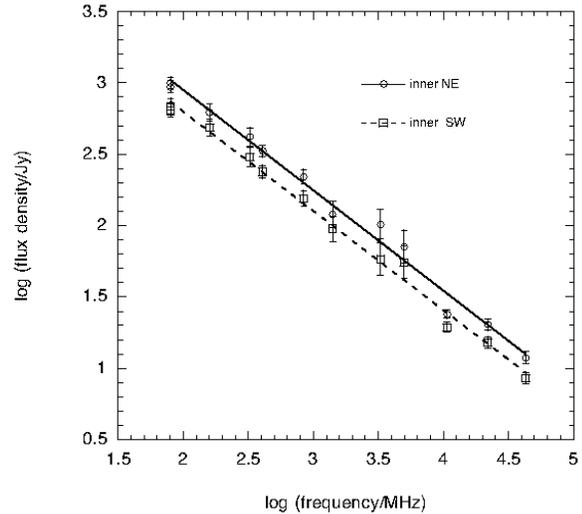
A most interesting feature in Fig. 2 is the lack of any spectral break. Except for the measurement of Harris & Roberts (1960) at 960 MHz, the best fit line passes through or touches the ends of the error bars. A flattening of the spectrum in the high frequency range could imply new ejections replenishing the highest energy electrons, while a steepening could imply losses; however, neither of these two effects is observed. Since the spectrum is straight, we submit that the electrons are undergoing some kind of continuous reacceleration.

3.2. The spectrum of the Inner Lobes

Table 2 lists the integrated flux densities of the individual ILs. The widest frequency range in which the spectral indices have been given is 18.3 to 5000 MHz, and the highest frequency at which the flux has been measured is 43 GHz. By collecting published fluxes we have produced a spectrum extending from 80 MHz to 43 GHz. The spectra of the individual ILs are shown in Fig. 3. The best fit lines give an index of -0.70 ± 0.02 for both ILs and correlation coefficients of 0.994 and 0.996 for the ILNE and ILSW, respectively. Thus, we confirm the results of Slee et al. (1983) who found -0.70 for both indices between 80 MHz and 10.7 GHz. We see that the fluxes of the ILNE are larger than those of the ILSW. The equality of the indices supports the hypothesis that the lobes were produced by electrons coming from a common population. Table 5 presents the spectral indices determined by different authors.

3.3. The spectrum of the Giant Outer Lobes

Even though a determination of the spectra of the individual Giant Outer Lobes is of much interest to understand the evo-

lution of this radio galaxy, their flux densities have been measured at only four frequencies: 408 and 1410 MHz by Cooper et al. (1965), 960 MHz by Bolton & Clark (1960), and 4670 MHz by Junkes et al. (1993). Furthermore their spectra have not been determined. We have added 2650 MHz by undertaking graphical integration of the brightness temperature contour maps published by Cooper et al. (1965) (see Table 3).

We have also repeated the calculations of Cooper et al. at 406 and 1410 MHz to ensure the use of the same criterion to separate the GLN, the GLS and the CR. The Northern Loop is not shown in the 5000 MHz map by Haynes et al. (1983) and for this reason these data have not been considered. In this study we have included the Northern Middle Lobe and the Northern Loop as parts of the GLN.

As mentioned earlier, the major problem at frequencies of 1410 MHz and below is the separation of the GLN from the CR which, due to lack of sufficient angular resolution, merges with the Northern Middle Lobe. This complication does not exist in the GLS because there is no southern counterpart of the Northern Middle Lobe and so the contours can be better estimated. In spite of these difficulties we believe that the separation can be achieved with reasonable accuracy thus: 1) by following the trend of the isophotes of the different components, 2) by assuming that the contours of the CR are symmetrically elongated, 3) by assuming that the GLN and GLS contours lie only north and south of the source's center declination, and 4) confirming that the sum of the fluxes of the three parts is close to the integrated flux obtained for the Whole Source. The flux densities and the spectra are shown in Table 3 and Fig. 4, respectively.

Cooper et al. (1965) apparently calculated the flux of the Whole Source at 960 MHz since they state that, with the Caltech flux density scale, the flux obtained by Bolton & Clark (1960) at the same frequency would come "closely into line with *our*

Table 5. Spectral indices of the Inner Lobes

ν range (MHz)	α_{ILNE}	α_{ILSW}	$\alpha_{\mathrm{both}}^{\mathrm{a}}$	Reference
$18.3 - 5000$			-0.64	Lockhart & Sheridan (1970)
$19.7 - 5000$			-0.6	Cooper et al. (1965)
$80 - 160$			-0.52	Slee (1995)
$80 - 10700$	-0.70 ± 0.02	-0.70 ± 0.02		Slee et al. (1983)
$80 - 43000$	-0.70 ± 0.02	-0.70 ± 0.02		This work[b]
< 150			-0.25	Lequeux (1962)[c]
> 150			-0.80	Lequeux (1962)[c]
$408 - 5000$			~ -0.6	Wall & Schilizzi (1979)
$1400 - 4900$	$\leq 0.86^{\mathrm{c}}$	$\leq 0.64^{\mathrm{d}}$		Burns et al. (1983)
$5000 - 31400$			-0.95	Geldzahler & Witzel (1981)

[a] Presumably includes both ILs.

[b] From collected data.

[c] Cited by Johnson (1963).

[d] For peak of centroids.
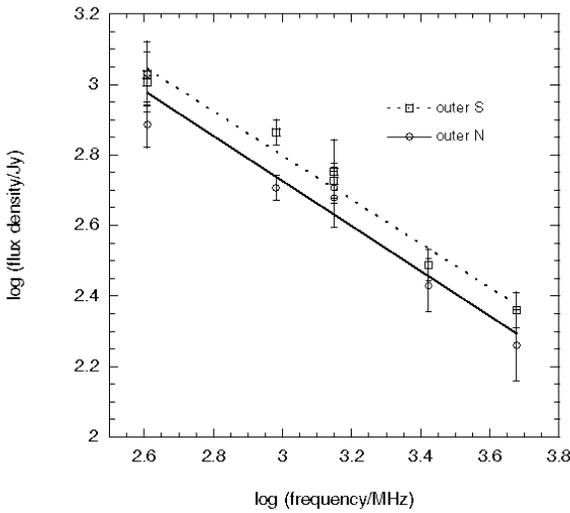
Fig. 4. Integrated flux density spectrum of the Giant Outer Lobes. The straight lines represent the least-squares fits to the data corresponding to the N and S lobes, given by the equations $\log S_{\mathrm{GLN}} = (4.64 \pm 0.21) - (0.64 \pm 0.07) \log \nu$ and $\log S_{\mathrm{GLS}} = (4.68 \pm 0.14) - (0.63 \pm 0.05) \log \nu$, respectively

own flux density at this frequency". However, this flux density is not given in their paper. From their map we have calculated a value of 1372 ± 11 Jy, which is well below the values given by both Bolton & Clark (1960) and Harris & Roberts (1960); see Table 1. Also, our flux determinations at 960 MHz for the GLN and GLS from the map of Cooper et al. (431 and 613 Jy, respectively) are below the 508 and 731 Jy determined by Bolton & Clark (1960). Interestingly, however, the flux ratios GLN/GLS are the same. We conclude, however, that the 960 MHz map of Cooper et al. (1965) has a large temperature scale offset, which we have not attempted to estimate. We do not consider these data further.

Our flux determinations at 1410 MHz are in agreement with those of Cooper et al. (1965). Also their GLS value at 406 MHz is in good agreement with ours. However, there is disagreement between the GLN fluxes (see Table 3). We believe this is due to the problem of separating the large scale components.

In Fig. 4 it is seen that, except for the 406-MHz determinations of Cooper et al. (1965), the mean value of the GLS is higher than that of the GLN at all frequencies. The best fit lines through the mean values of the GLS and GLN give spectral indices of -0.63 ± 0.05 and -0.64 ± 0.07, respectively. Thus, the spectral indices are equal, within the precision of the fit. The correlation coefficients for these data are 0.987 and 0.972, respectively.

The average spectral indices of the Whole Source (-0.70 ± 0.01) and of the ILs (-0.70 ± 0.02) are considerably more reliable than those of the GLs because they were obtained in a much wider frequency range and with a significantly larger number of data. This is reflected in the high correlation coefficients: 0.998 (Whole Source), 0.994 (ILNE), and 0.996 (ILSW). However, the spectral indices of the GLs have been determined in a narrower range of frequencies, with smaller number of measurements and data with larger error bars due to the difficulty in separating the CR from the GLs. Since the GLs contribute 73% of the luminosity of the Whole Source (see Sect. 3.4) we would expect the spectral index of the GLs to be very close to that of the Whole Source. For both GLs the errors of fit make this expectation possible.

In the search for the spectral indices of the individual GLs, we have used the work of Combi & Romero (1997) who studied the spatial distribution of the spectral index over the source at both 408 and 1410 MHz. From a graphical integration of their Fig. 2 we have deduced averaged indices of -0.75 and -0.70 for the GLN and GLS, respectively. To separate the lobes in their figure we arbitrarily drew a constant declination line through $-43.7°$, which is the declination of the center of the source. The mean error of ± 0.08 in the map of indices, quoted by the original authors, is sufficient to bring the values we computed into agreement with the indices discussed earlier. Table 6 shows the spectral indices of the Giant Outer Lobes.

Table 6. Spectral indices of the Giant Outer Lobes

ν range (MHz)	α_{GLN}	α_{GLS}	α_{both}	Reference
$18.3 - 85.5$			-1.25	Shain (1958)
$408 - 1410$	$-0.75^{\mathrm{a}} \pm 0.08^{\mathrm{b}}$	$-0.70^{\mathrm{a}} \pm 0.08^{\mathrm{b}}$		This work[c]
$408 - 4750$	-0.64 ± 0.07	-0.63 ± 0.05		This work
$408 - 5000$			~ -0.9	Wall & Schilizzi (1979)

[a] Averaged over spatial distribution.
[b] Errors quoted by original authors.
[c] Based on data from Combi & Romero (1997).

In their review, Ebneter & Balick (1983) state that "the spectral index of the northern lobe is noticeably different from that in the southern lobe"; however, they give no measurements or references.

Examining the spectral indices of the ILs and GLs we see that they are similar. This precludes the idea, sustained by some authors, that the outer lobes are a sort of halo since this would be expected to have a much steeper spectrum. For example, Shain (1958) noticed a difference in the spectrum of the extended and central sources, with indices of -1.25 and -0.6, respectively, and interpreted that "...the very high frequency observations refer only to the central source...". This is disclaimed by our findings. The similarity of the spectral indices of the ILs and GLs also supports the hypothesis that the pairs of lobes were formed by two energetic electron ejections. These ejections may have come at different times from the same electron parent population or, if the electrons were generated at the time of the ejection, the mechanism produced the same distribution of energies.

3.4. Luminosities

Table 7 presents the luminosities of the analyzed Cen A components. To compute these luminosities we have assumed that the power law spectra fitted to the mean values of the data, as shown in Figs. 2, 3 and 4, are valid between 4.7 MHz and 43 GHz. This may not be so for the GLs at high frequencies nor for the ILs at low frequencies; ranges where there are no data. If the assumption is not valid the consequences would be more noticeable for the GLs, since the luminosity for a power law spectrum with a negative index is determined by the high-frequency end (when the two ends are distant). We are also assuming that the power is radiated isotropically. The adopted distance of 3.5 Mpc is the most recent value we have found (Hui et al. 1993). We have not applied K corrections since the redshift is only 0.002.

Table 7 shows several interesting results. The GLs contribute with 73% of the total luminosity while the contribution of the ILs is 18%; that is, the GLs are four times more luminous than the ILs. Taking the luminosities in Table 7 at face value, the Nuclear Region contributes approximately 10% of the total luminosity. It is seen that, of the GLs, the southern one is the more luminous while the opposite is true of the ILs; the ratio of luminosities are ILSW/ILNE=0.68 and GLS/GLN=1.20. It is interesting that, in spite of the fact that these luminosity ratios are neither unity nor

Table 7. Luminosity between 4.7 MHz and 43 GHz

Component	L $(10^{40}$ erg s$^{-1})$
Whole Cen A	23.9
Outer lobe N	7.9
Outer lobe S	9.5
Inner lobe NE	2.5
Inner lobe SW	1.7
Nuclear region	2.3

close to it, the spectral indices of each pair are the same. In the double ejection hypothesis this could imply that, in both epochs, the fast electrons came from the same parent population but that either the amounts or the densities of ejected particles, were different. Further, the numbers of ejected particles were different not only in the first and second ejections, but also between the two opposing jets. The fact that the much older GLs have maintained their original spectral indices, at least up to 4.75 GHz, indicates that they have not suffered significant losses.

In the literature we have found very few calculations related to the luminosity of Cen A. Burbidge & Burbidge (1957) assumed a core-halo structure with three different spectral indices between 18 and 3000 MHz, and a distance of 2.5 Mpc, obtaining 10^{40} erg s^{-1}. Moffet (1975) quotes $5.0 \ 10^{41}$ erg s^{-1} between 10 MHz and 10 GHz, and gives no indication of the spectrum, while Rogstad & Ekers (1969) give $3.5 \ 10^{41}$ erg s^{-1} between 10 MHz and 100 GHz, for a distance of 4 Mpc and an unspecified spectrum. Matthews et al. (1964) find $7.4 \ 10^{41}$ between 10 MHz and 100 GHz, adopting a distance of 4.7 Mpc. We have discussed elsewhere (Alvarez et al. 1993) the dangers of computing luminosities from data over a short range of frequencies, at a single frequency or, even worse, assuming a spectral index for the whole spectrum. Considering this, and the different distances and frequency ranges adopted, the above values are consistent. The luminosities of Table 7 are reduced by one half if computed up to 4.75 GHz rather than 43 GHz.

3.5. Spectral aging

We have seen that the spectra of the GLs and ILs are straight over all the observed range of frequencies up to 4.75 and 43 GHz, respectively. We can estimate upper limits to the ages of the

fast electrons responsible for the lobes if we assume, first, that their spectra break down precisely at 4.75 and 43 GHz, though there are no observations to see the steepening, and second, that only synchrotron and inverse Compton losses occur above those frequencies. Following Perola (1981), the age, in years, is given by:

$$t_{\rm r} = 2.6\,10^4 \frac{\sqrt{B}}{(B^2 + B_{\rm r}^2)\sqrt{\nu_{\rm b}(1+z)^2}} \,, \tag{1}$$

where B is the magnetic field strength in the source (G), $B_{\rm r}$ is the equivalent magnetic field (G), $\nu_{\rm b}$ is the break frequency (Hz), and z is the cosmological redshift. For the cosmic microwave background $B_{\rm r} = 3.2\,(1+z)^2\,\mu$G; the multiplying constant is derived by taking a radiation energy density of $4.1\,10^{-13}$ erg s^{-1}. For Cen A we will assume $z = 0$.

The magnetic field strength has been inferred from x-ray observations. For the GLs, Cooke et al. (1978) and Harris & Grindlay (1979) give 0.7 and $0.6\,\mu$G, respectively, while Marshall & Clark (1981) give $B > 1.6\,\mu$G. These authors assume that one and the same distribution of relativistic electrons produces the x-ray emission by inverse Compton mechanism and radio emission by the synchrotron process. They take special care to remove the contribution from the Central Region. Feigelson & Berg (1983) do not detect x-ray emission neither from the GLs nor from the ILs, and estimate that the field in the GLs and ILs must be larger than 1.6 and $3\,\mu$G, respectively. From minimum pressure arguments, Burns et al. (1983) obtain 12 and $13\,\mu$G for the ILNE and ILSW, respectively. The corresponding ages are $5.8\,10^6$ and $5.6\,10^6$ years. It should be noted that these calculations refer only to the *centroids* of the ILs.

Eq. (1) is doubled-valued for B, that is, for each $t_{\rm r}$ there are two Bs that satisfy it, except for $B = B_{\rm r}/\sqrt{3} = 1.85\,\mu$G, where a maximum of $37\,10^6$ years occurs for $t_{\rm r}$ (assuming $z = 0$).

Adopting for the GLs $B = 0.7\,\mu$G and $\nu_{\rm b} = 4.75$ GHz we obtain that their ages are less than $28\,10^6$ years. For the ILs with $B = 3\,\mu$G and $\nu_{\rm b} = 43$ GHz the upper limit for the age yields $11\,10^6$ years. The estimated maximum ages are of the same order of magnitude than those found by Mack et al. (1998) for giant radio galaxies, and by Feretti et al. (1998) for tailed radio galaxies.

Because of the way the x-ray workers computed the magnetic field, it is reasonable to use Eq. (1) complete. Had we assumed only synchrotron losses ($B_{\rm r} = 0$) the upper limits for the GLs and ILs would have been $58\,10^7$ and $24\,10^6$ years, respectively. We see that the presence of inverse Compton losses can make a large difference in the estimation of ages. Future radio observations at frequencies higher than the actual break frequencies should reveal the shape of the spectrum and should give information about the radiating mechanism.

We can calculate the equipartition field, $B_{\rm eq}$. This is given by Perola (1981), in c.g.s. units, by:

$$B_{\rm eq} = [4.5\,(1+K)\,{\rm c}\,L]^{\frac{2}{7}}\,f^{-\frac{2}{7}}\,R^{-\frac{6}{7}}\,, \tag{2}$$

where K is the ratio of relativistic protons to relativistic electrons, c is a constant that depends on the radio spectral index and

on the frequencies between which the luminosity L is calculated (Pacholczyk 1970), $f(\leq 1)$ is a filling factor, and R is the radius of the source. We will assume $K = 0$ and $f = 1$. For the GLs we have calculated c for $\alpha = -0.70$ and for the end frequencies 4.7 and 4750 MHz, obtaining $7.7\,10^7$. We have adopted an angular size of $5°$ which, assuming a spherical source, gives a radius of 320 kpc. Finally, from Table 7 we obtain the luminosities. In the case of the GLs the given luminosity should be divided approximately by 2 because the known spectrum extends only up to 4.75 GHz. For each of the ILs we have adopted an angular extent of $5'$ and end frequencies 4.7 MHz and 43 GHz, while c $= 4.4\,10^7$ for $\alpha = -0.70$. With these numbers we obtain $B_{\rm eq} = 0.4\,\mu$G and $1.2\,\mu$G for the GLs and ILs, respectively. We see that the values adopted for the magnetic field in our estimations of age are of the same order of magnitude as those derived from equipartition arguments.

3.6. P-α correlation

Extended extragalactic structures have been divided by Fanaroff & Riley (1974) into two luminosity classes. The weaker sources brightest at the center and fading toward the edge are defined as FRI class. The more luminous sources are limb-brightened and are defined as FRII class; they often show hot-spots at the farthest edges of the structure. For powerful, extended, double radio galaxies, Laing & Peacock (1980) found a correlation between radio luminosity (defined by them as P) at 1400 MHz and spectral index, and also between redshift (z) and spectral index. The correlation holds for FRI sources and for the extended structure of FRII sources, observing a smooth continuity between the two classes in the P-α diagram. Even though Cen A cannot be considered as a powerful radio galaxy, its luminosity is within the range of the sample selected by Laing & Peacock (1980), so we can use it to check the correlation. We have found that Cen A fits quite well the P-α correlation, as illustrated in Fig. 3 of Laing & Peacock (1980), which contains all identified sources in the 178 MHz sample (with the central source *not* removed). Originally, there was some uncertainty as to whether the real correlation was with the luminosity or with the redshift; however, Gopal-Krishna (1988) has given evidence that the correlation is primarily with radio luminosity. Since the lowest z in the Laing & Peacock's sample is 0.03, the much smaller z of Cen A (0.002) offers a good opportunity to test the z-α correlation. We have found that Cen A definitely does not fit this correlation, in support of Gopal-Krishna's (1988) result.

4. Conclusions

We have presented and discussed the integrated flux density spectrum of the large-scale Cen A components. To obtain the spectra we have resorted to three types of data: i) our own observations at 45 MHz, ii) results deduced by us from data found in the literature, and iii) results obtained by other authors. In this way we have studied the spectra in extended frequency ranges, resolving controversies about the spectral index of the Whole

Source and presenting, for the first time, the spectra of the individual Giant Outer Lobes.

The conclusions are as follows:

1. We have obtained the total integrated spectrum of the whole of Cen A using data of types i, ii and iii. At 45 MHz we have used our own observations and determined a flux density of 14900 ± 2200 Jy. The spectrum between 10 and 4750 MHz is fitted well by a power law of index -0.70 ± 0.01. This result belies a spectral break reported by other authors in the past.

2. Using data of types ii and iii we have determined, for the first time, the spectra of the individual Outer Giant Lobes between 406 and 4750 MHz. The North and South lobes fit *the mean values* with power laws of indices -0.64 ± 0.07 and -0.63 ± 0.05, respectively. That is, the spectral indices are practically equal.

3. We have obtained the individual spectra of the Inner Lobes using data of type iii. Between 80 MHz and 43 GHz, the Northeastern and Southwestern lobes' fluxes are fitted well by a power law of index -0.70 ± 0.02. This results confirm that of Slee et al. (1983) obtained over a smaller frequency range.

4. We have calculated the luminosities of the Whole Source, GLs and ILs, assuming that their spectra, determined from mean values, follow power laws between 4.7 MHz and 43 GHz. A distance of 3.5 Mpc was adopted. We have found that the GLs are four times more luminous than the ILs and that the luminosity ratio GLS/GLN is 1.20, while the corresponding ratio ILSW/ILNE is 0.68. The total luminosity of Cen A is $23.9 \, 10^{40}$ erg s^{-1}.

5. Since the GLs contribute 73% of the luminosity of the Whole Source we would expect the index of the GLs to be very close to that of the Whole Source. The errors in the fit of the GLs make this expectation possible.

6. The similarities between the spectral indices of the GLs and ILs support the hypothesis that the structure was formed by two successive ejections from the same parent population of relativistic electrons, or from two different populations generated at the time of ejection with the same energy spectrum. Differences in the luminosities between the ILs and between the GLs could be attributed to differences in electron ejection densities. The fact that there is no noticeable steepening at the high frequency end could indicate that the object is young, or that there is reacceleration or continuous ejection.

7. Assuming only synchrotron and inverse Compton losses, the GLs and ILs are younger than $28 \, 10^6$ and $11 \, 10^6$ years, respectively.

8. We have shown that Cen A supports the P-α rather than the z-α correlation.

References

Alvarez H., Aparici J., May J., Navarrete M., 1993, A&A 271, 435

Alvarez H., Aparici J., May J., Olmos F., 1994, Experimental Astronomy 5, 315

Alvarez H., Aparici J., May J., Olmos F., 1997, A&AS 124, 315

Baars J.W.M., Genzel R., Pauliny-Toth I.I.K., Witzel A., 1977, A&A 61, 99

Bolton J.G., Clark B.G., 1960, PASP 72, 29

Bracewell R.N., 1962, Radio Astronomy Techniques. In: Flügge S. (ed.) Handbuch der Physik 54, Springer, Berlin, p. 119

Burbidge G.R., Burbidge E.M., 1957, ApJ 125, 1

Burns J.O., Feigelson E.D., Schreier E.J., 1983, ApJ 273, 128

Cameron M.J., 1971, MNRAS 152, 403

Christiansen W.N., Frater R.H., Watkinson A., O'Sullivan J.D., Lockhart I.A., 1977, MNRAS 181, 183

Combi J.A., Romero G.E., 1997, A&AS 121, 11

Cooke B.A., Lawrence A., Perola G.C., 1978, MNRAS 182, 661

Cooper B.F.C., Price R.M., Cole D.J., 1965, Aust. J. Phys. 18, 589

Day G.A., Caswell J.L., Cooke D.J, 1972, Aust. J. Phys. Suppl. 25, 1

Ebneter K., Balick B., 1983, PASP 95, 675

Ellis G.R.A., Hamilton P.A., 1966, ApJ 143, 227

Fanaroff B.L., Riley J.M., 1974, MNRAS 167, 31

Feigelson E.D., Berg C.J., 1983, AJ 269, 400

Feretti L., Giovannini G., Klein U., et al., 1998, A&A 331, 475

Geldzahler B.J., Witzel A., 1981, AJ 86, 1306

Goldstein S.J., 1962, AJ 67, 171

Gopal-Krishna, 1988, A&A 192, 37

Hamilton P.A., Haynes R.F., 1968, Aust. J. Phys. 21, 895

Harris D.E., Grindlay J.E., 1979, MNRAS 188, 25

Harris D.E., Roberts J.A., 1960, PASP 72, 237

Haslam C.G.T., Klein, U., Salter C.J., et al., 1981, A&A 100, 209

Haslam C.G.T., Salter C.J., Stoffel H., Wilson W.E., 1982, A&AS 47, 1

Haynes R.F., Cannon R.D., Ekers R.D., 1983, Proc. ASA 5, 241

Heeschen D.S., 1960, ApJ 133, 322

Hill E.R., 1968, Aust. J. Phys. 21, 735

Hui X., Ford H.C., Ciardullo R., Jacoby G.H., 1993, ApJ 414, 463

Israel F.P., 1998, A&AR 8, 237

Johnson H.M., 1963, Publ. NRAO 1, 251

Jones P.A., McAdam B., 1992, ApJS 80, 137

Junkes N., Haynes R.F., Harnett J.I., Jauncey D.L,. 1993, A&A 269, 29

Kraus J.D., 1966, Radio Astronomy. McGraw-Hill, New York, p. 87

Laing R.A., Peacock J.A., 1980, MNRAS 190, 903

Lequeux J., 1962, Comptes Rendue 255, 1865

Little A.G., Cudaback D.D., Bracewell R.N., 1964, Proc. Nat. Acad. Sci. 52, 690

Lockhart I.A., Sheridan K.V., 1970, Proc. ASA 1, 344

Mack K.H., Klein U., O'Dea C.P., Willis A.G., Saripalli, L., 1998, A&A 329, 431

Marshall F.J., Clark G.W., 1981, ApJ 245, 840

Matthews T.A., Morgan W.W., Schmidt M., 1964, ApJ 140, 35

May J., Reyes F., Aparici J., et al., 1984, A&A 140, 377

McGee R.X., Slee O.B., Stanley G.J., 1955, Aust. J. Phys. 8, 347

Moffet A.T., 1975. In: Sandage A., Sandage M., Kristian J. (eds.) Galaxies and the universe. The U. of Chicago Press, Chicago, p. 21

Pacholczyk A.G., 1970, Radio Astrophysics. Freeman, San Francisco, p. 233

Perola G.C., 1981, Fund. Cosmic Phys. 7, 59

Price K.M., Stull M.A., 1973, Nature Phys. Science 245, 83

Rogstad D.H., Ekers R.D., 1969, ApJ 157, 481

Roman N., Haddock F.T., 1956, ApJ 124, 35

Shain C.A., 1958, Aust. J. Phys. 11, 517

Shain C.A., 1959. In: Bracewell R.N. (ed.) IAU/URSI Paris Symposium on Radio Astronomy. Stanford U. Press, Stanford, p. 328

Sheridan K.V., 1958, Aust. J. Phys. 11, 400

Slee O.B., 1995, Aust. J. Phys. 48, 143

Slee O.B., Sheridan K.V., Dulk G.A., Little, A.G., 1983, Proc. ASA 5, 247

Smith R.M., Bicknell G.V., 1986, ApJ 308, 36

Sofue Y., Reich W., 1979, A&A 38, 251

Tateyama C.E., Strauss F.M., 1992, MNRAS 256, 8

Wall J.V., Schilizzi R.T., 1979, MNRAS 189, 593